Paper 83

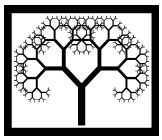

Proceedings of the Third International Conference on Railway Technology: Research, Development and Maintenance, J. Pombo, (Editor),
Civil-Comp Press, Stirlingshire, Scotland.

Validation of the Design of the Torque Limiter of the AIR Wheelset on the Sardinian Backbone Network

A. Bracciali and G. Megna
Dipartimento di Ingegneria Industriale
Università di Firenze, Italy

Abstract

A new wheelset design has been recently developed where independent wheels rotating on roller bearings are connected by a coaxial transmission shaft. The wheels-shaft connection can be done using a torque limiter, enabling a substantial reduction of the longitudinal forces and therefore a possible reduction of wear and RCF problems on both wheels and rails. This paper presents a study of the feasibility of a possible torque limiter design, crucial in the success of the aforementioned wheelset, by using a mission profile based on the mixed-conditions typical of the Sardinian backbone network.

Keywords: AIR wheelset, torque limiter, Sardinia, simulation.

1 Introduction

A new wheelset design, named *Apparently Independently Rotating Wheels Wheelset*, or *AIR Wheelset* for short, based on independently rotating wheels torsionally connected through a torsionally stiff shaft, has been recently patented [1]. It is extensively described in ref. [2], while vehicle dynamics implications are described in ref. [3], contact mechanics issues are described in ref. [4] and maintainability issues are described in ref. [5]. A thorough analysis of the current wheelset design is reported in the review paper [6] given at this conference as an opening lecture. Although the reader is referred to these papers for more details, a sketch of the *AIR wheelset* is shown in Figure 1.

The arrangement consists of two wheels equipped with bearings and brake discs that are connected through a torsionally rigid shaft. The development of the *AIR Wheelset* was originated by the search of a better maintainable wheelset (wheels can be changed rapidly) and an improved safety (the axle is not present anymore).

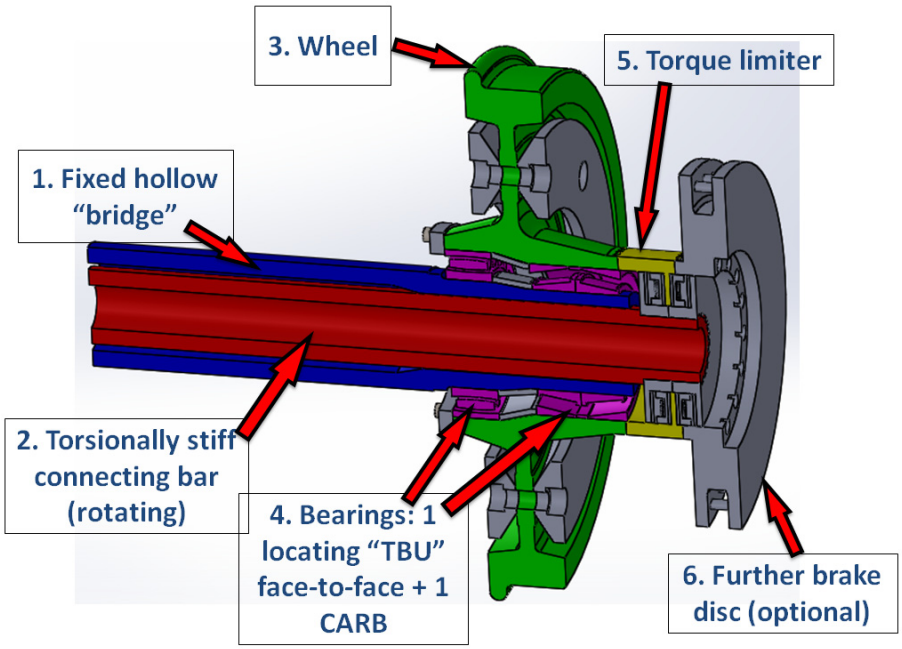

Figure 1: Sketch of the *AIR Wheelset*. The torque limiter described in this paper is rather different (see par. 4).

One of the possible versions of this wheelset is equipped with torque limiters which allow the wheels to rotate relatively in tight and mild radius curves. The central idea of the use of the torque limiters is to reduce the longitudinal forces to a predefined value, while keeping the behaviour in straight track exactly the same as that for a conventional wheelset.

The design of the friction torque limiter is therefore central to the success of the *AIR Wheelset*. The correct value of the maximum transmissible torque must be properly set in order to intervene correctly by at same time limiting the clutch wear and to get the best results in terms of protection from corrugation and RCF defects.

This paper proposes a design for the torque limiter and evaluates its behaviour in a mixed mission profile, with a mixture in tangent track, mild and sharp curves.

2 Simulation of the mission profile on the Sardinian backbone line

A few years ago, one of the authors was engaged by the regional government of Sardinia to evaluate the mission profile of a new family of tilting trains to be used on the backbone of the Sardinian railway network. The goal of the local government was to achieve a running time as close as possible to two hours between Cagliari and Sassari, i.e. the largest cities in Sardinia. Running times were calculated for different rolling stocks with a time-step integration (Δt=0.5 s) considering the following conditions:

- rolling stock manufacturers provided traction curves (mechanical characteristic, i.e. available tractive effort vs. speed) as well as train resistance vs. speed;
- curvature resistance was calculated according to Italian Infrastructure Manager (RFI) provisions;
- the prescribed stops were included considering appropriate decelerations according to the Italian signalling system;
- braking effort (braked mass percentage) was appropriately included in long descents (drag braking), checking the effect of hydraulic braking.

The Sardinian backbone (Figure 2) is a Y-shaped line. For convenience the line was split in three sections during simulations, as follows:

- Section 1, Northbound: Cagliari-Oristano-Chilivani, in common with the other sections;
- Section 2, North-Eastbound: Chilivani-Olbia;
- Section 3, North-Westbound: Chilivani-Sassari.

Figure 2: The Sardinian railway network. Sections described in this paper: in red, Section 1 (Cagliari-Oristano-Macomer-Chilivani), in green, Section 2 (Chilivani – Olbia), in yellow, Section 3 (Chilivani-Sassari).

The southernmost section leaves from Cagliari and is straight up to Oristano, then the line is particularly winding and steep to Macomer before and to Chilivani afterwards, where the lines from Olbia and Sassari join.

Section 1 properties are shown in Figure 3. It can be seen that the line is nearly flat (slope $i < 10$ ‰) between Cagliari and Oristano, with many straight subsections and mild curves with $r > 900$ m. Line speed (limited by signalling) is 150 km/h. The subsection from Oristano to Chilivani through Macomer is winding and steep, with slopes up to 26 ‰ and tight curves with radii down to $r = 300$ m.

For space reasons no similar figures for the other sections are shown in this paper. The remaining of the paper will focus therefore on Cagliari-Olbia line, including Section 1 and Section 2. No main differences were found applying what follows to the route Cagliari-Sassari (Section 1 + Section 3), which is shorter and less meaningful than the one selected.

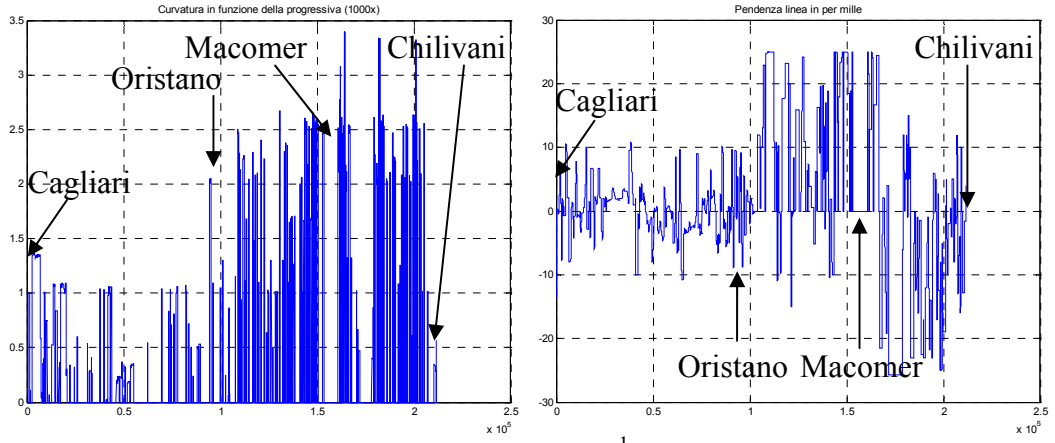

Figure 3: Section 1 properties. Curvature [km^{-1}] (left) and Northbound slope [‰] (right). Abscissa: distance in [m]. Oristano is at km 94.1, Macomer is at km 153.8.

3 Running conditions and dissipated energy

3.1 Hypotheses and limitations

The estimation of the torque acting on axles of the front bogie is derived from [3] and [4]. These simulations were conducted on the "ERRI wagon", a library vehicle available in the running dynamics software package VI-Rail 16.0 and therefore, strictly speaking, they are applicable only to this vehicle. On the other side, running time simulations in Sardinia were performed on a DMU vehicle with possibly completely different suspension arrangement.

Nevertheless, it is believed that the selected limiting torque of 4000 Nm is due to the relatively high yaw stiffness of the ERRI wagon (that is stable with new profiles up to speeds greater than 100 m/s even with relatively poorly performing anti-yaw

dampers) and that with more modern vehicle designed to run at much lower speeds the torque could be set at a much lower value. The calculations presented here are therefore possibly largely overestimated in terms of dissipated energy. The estimation of torque limiter life is therefore precautionary.

3.2 Influence of running conditions on torque and dissipated power

The torque T acting on the first and the second axle was estimated from a linear interpolation of the curves given in [3], in which single values were obtained for each combination of a set of curve radii (300, 548, 1000, 1430, 2000, 3300 m) and non-compensated accelerations (-1, 0, +1 m/s^2), always with 160 mm cant. The curves exhibited sufficient regularity and the linear interpolation was considered sufficient to capture at least the order of magnitude of torques and powers involved in the dissipation process.

Instantaneous dissipated power is calculated as $max(|T(t)|\text{-}T_{lim},0)\cdot|\Delta\omega(t)|$, i.e. where the torque limiter is active resulting in a constant torque of T_{lim}=4000 Nm. Clearly no power is dissipated when torque is $T<T_{lim}$.

The resulting maps are shown in Figure 4. It can be seen that the maximum power is lower than 2.5 kW and is reached for mild curves (1000-1430 m radius) and high non-compensated acceleration values (+1 m/s^2). Although (negative) torques are greater on the second axle, power is limited as speed for small curve radius is limited. The peak power on second axle is therefore slightly less than 1 kW.

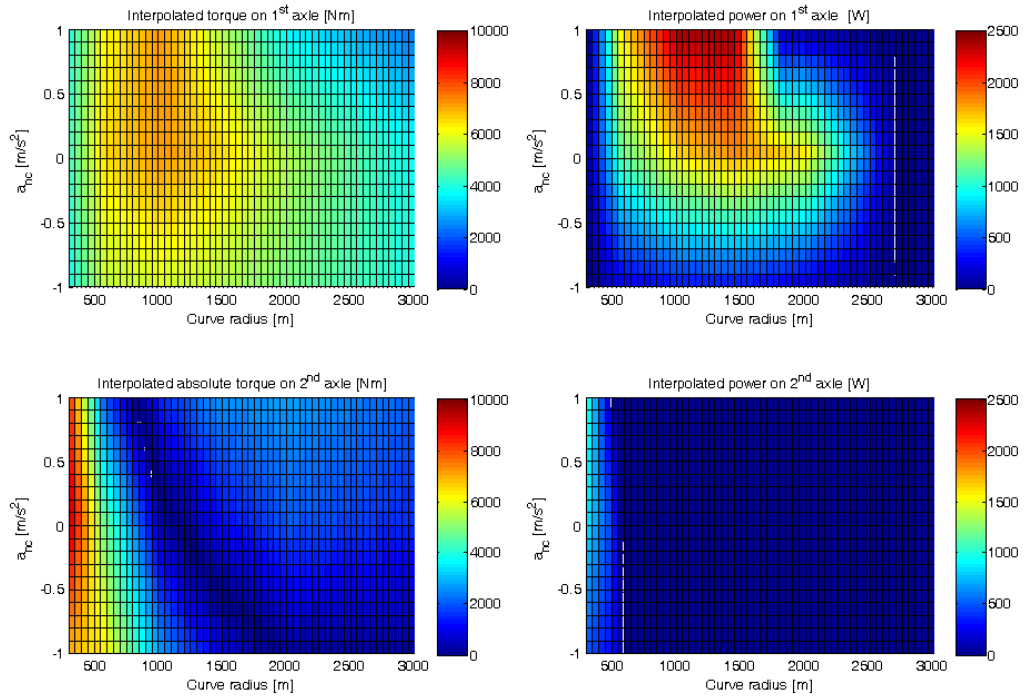

Figure 4: Interpolated torques (left) and resulting powers dissipated in the torque limiter (right). Torque on second axle shown in absolute value.

3.3 Cumulative energy dissipated in the torque limiter

In the Sardinian backbone line the maximum achievable non-compensated acceleration a_{nc}=1 m/s^2 is reached regularly (Figure 5).

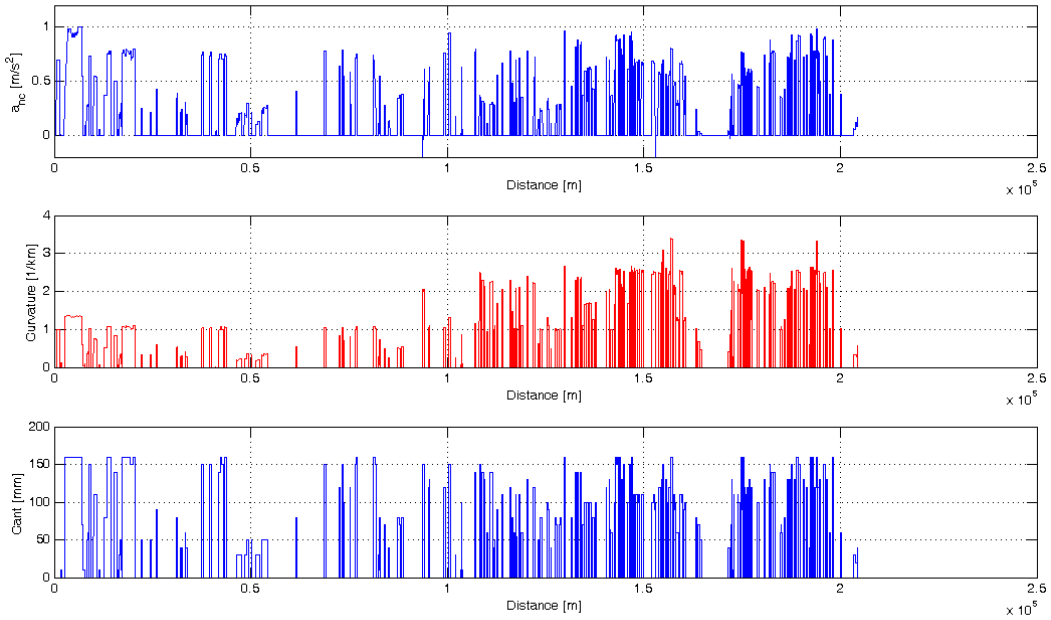

Figure 5: Resulting non-compensated acceleration (top) on Section 1 according to the mission profile and line characteristics, i.e. curvature (mid) and cant (bottom).

Nevertheless, the actual energy dissipated in the torque limiter depends on the mission profile, in terms of line properties (radius, cant) and running conditions (speed). It is evident that completely different results can be obtained by changing the mission profile. One of the authors discovered, for example, that in another application [7] the maximum non-compensated acceleration was consistently below 0.5 m/s^2 to reduce rail wear under heavy traffic.

Once the kinematic quantities of interest are calculated, they can be combined with the torque limitation setting to obtain the information shown in Figure 6 for Section 1. It can be seen that the front axle limiter intervenes much more frequently (mild curves at higher speeds) while the one on the second axle intervenes only in the more curvy portion of the lines, with sharper curves run at lower speed. As a result, in Section 1 the front limiter dissipates around 2.5 MJ, while the rear limiter dissipates around 0.4 MJ.

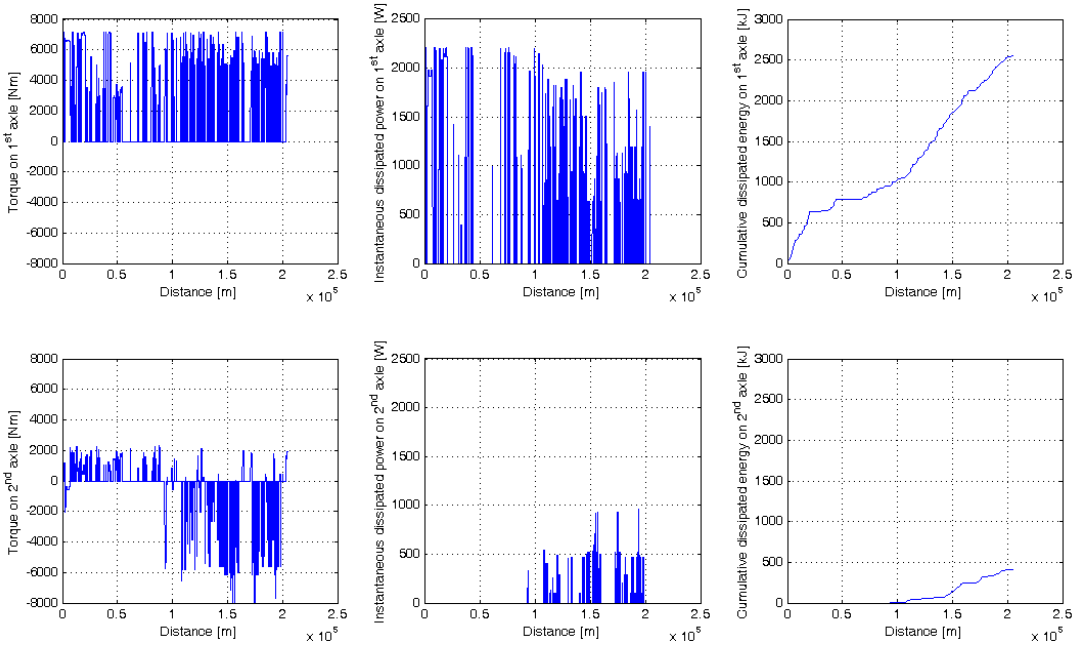

Figure 6: Instantaneous torque (left), instantaneous power (mid) and cumulative dissipated energy (right) on Section 1 for the first (top) and the second (bottom) axle.

Adding the energy on Section 2, the overall dissipated energy in the line Cagliari-Olbia can be evaluated in around 3.7 MJ on the front axle and 0.7 MJ on the rear axle for a total trip of 276.8 km. Supposing that the two values swap when reversing the travelling direction, this leads to a total energy of 4.41 MJ for both the wheelsets on a 553.6 km trip. For reasons that will be evident later, the dissipated energy is expressed as the product of a *sliding* force in kN by a distance in km as follows: E_d = 4.41 MJ = 4.41 kN*km.

4 Torque limiter design

4.1 Make or buy?

As the design of the *AIR Wheelset* is already rather complex, the first idea was to adapt an off-the-shelf torque limiter. This unfortunately proved impossible because a deep market analysis didn't show any torque limiter with the desired characteristics. Commonly available torque limiters have in fact the following properties:

- as they normally don't have to be mounted on vehicles, their size is large and generally incompatible with low space available and low allowable (non-suspended) mass;

- their scope is to intervene quite rarely to protect a machinery from an exceptional case or a strange situation, while the torque limiter for the AIR wheelset has to intervene very frequently;
- torque limiters often disengage completely and require the intervention of an operator to reactivate the connection, something which is not compatible with the AIR wheelset application;
- even in the case of friction limiters, the difference in the angular speed of the motor and the driven shaft is normally rather large (e.g. the driven shaft is blocked and the motor continues to run at full speed), possibly "burning" the torque limiter soon if the situation is not fixed or restored;
- on the opposite, in the AIR wheelset the relative angular speed is very limited ($\Delta\omega_{max}$ = 0.62 rad/s = 5.92 rpm) and this leads to the small dissipated power values seen above ($P_{max} = \Delta\omega_{max}\ T_{max}$= 0.62*4000 = 2480 W), so no thermal problems arise;
- natural cooling provided by airflow around the torque limiter allows to consider the dissipative process as happening at ambient temperature;
- durability of the torque limiter is indeed a central factor, as it is expected that the torque limiter lasts for some million km before been serviced.

All these considerations led to the conclusion that a new torque limiting device had to be designed, and this is the object of this paper.

4.2 Description of the torque limiter

The torque limiter specifications were quite stringent. The only known characteristics was the intervention torque (4000 Nm), while all other boundary conditions had to be defined.

The design process was quite long and difficult, mainly because a fully passive solution was looked for in order to keep the philosophy of the *AIR wheelset*, that is an "all steel" solution without mechatronics or, in general, any closed-loop control strategy.

Figure 7 shows the designed compact and lightweight torque limiter. It is based on two steel coaxial rotors, one connected to the wheel of the *AIR wheelset* and the one connected to the internal shaft, that are both in contact with two spheroidal graphite (nodular) cast iron tapered discs, said "cones" (30° opening angle). These are pushed laterally by preloaded springs, whose force (22.5 kN) is sufficient to generate the desired torque (4000 Nm) under the hypothesis that the cast iron / hard steel friction coefficient is 0.23. This value is the minimum value found in the literature, so the calculation is conservative.

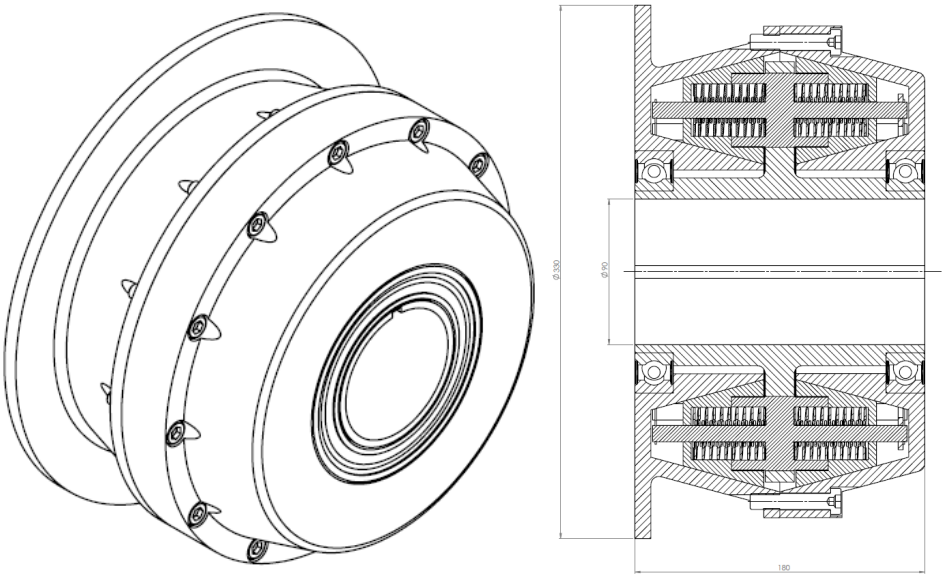

Figure 7: Torque limiter design. Axonometric view (left) and cross section (right).

4.3 Stick-slip considerations

Whenever a surface slides on another surface the well-known phenomenon of stick-slip may appear. This is particularly likely for high pressures (micro welds possible on similar materials) and low speeds (static friction coefficient much greater than kinetic friction coefficient). Although this is not the place to discuss stick-slip in detail, the phenomenon can be described by the model shown in Figure 8.

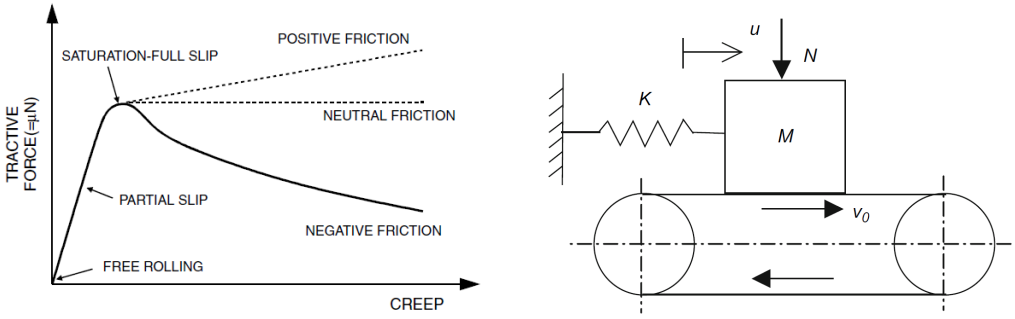

Figure 8: Friction-creepage curve with a negative slope after the adhesion limit (left, [8]); a simple mechanism where stick-slip occurs (right, [9])

Two conditions are necessary for the stick-slip phenomenon to occur: a relatively low stiffness K and a negative slope of the friction curve. Although only an experimental assessment can validate the design of the torque limiter, there are three independent conditions that may reduce or eliminate the onset of stick-slip:

- the stiffness of the connecting shaft, dictated by running dynamics conditions [3], is relatively high (≅ 1.35 MNm/rad);

- the use of spheroidal graphite cast iron cones make them less prone to stick-slip than grey cast iron under high-pressure and low-speed conditions;
- the natural presence of high axlebox vibrations level may have a positive impact, "shaking" the device and helping to win the breakout friction.

4.4 Estimated torque limiter life

As anticipated, the durability of the torque limiter is a central parameter for the success of design of the torque limiter, in order to guarantee a service time compatible with the maintenance schedule of the vehicle. Wear rate of the cones was estimated using the Archard's wear law

$$W = K_{ad} \frac{F_N}{H} \tag{1}$$

where W is the volume of worn material for unit of sliding distance between the bodies in contact [m^3/m], K_{ad} is the *adhesive wear coefficient* [-], F_N is the *normal contact force* [N] and H is *hardness* [N/m^2] of the softest material in contact. The rate K/H is also called *specific wear coefficient* (K_a) [m^2/N=m^3/J] and its value for different material is reported in Figure 9, together with the corresponding hardness.

Material	**Typical hardness range [kg/mm^2]**	**K_a coefficient [m^2/N]**
Low carbon steel	100-150	$\approx 5*10^{-13}$
Medium carbon steel	150-300	$\approx 10^{-13}$
High carbon steel	300-600	$\approx 5*10^{-14}$
Tool steel	600-850	10^{-15} - 10^{-14}
Nitrided steel	900 (surface)	$\approx 5*10^{-15}$
Grey cast iron (pearlitic / martensitic)	300-500	$3*10^{-16}$ - $5*10^{-14}$
Bronze	300-400	10^{-15} - 10^{-14}
Aluminium alloys	100-250	$\approx 10^{-13}$ ($\approx 5*10^{-12}$)
Hard chrome (cladding)	900-1000	$\approx 5*10^{-16}$
WC-Co	1000-1600	$\approx 5*10^{-16}$
Ni-P/SiC	800-900	$\approx 6*10^{-16}$
Polymer	10-100	10^{-15} - 10^{-14}
Reinforced polymers		$2*10^{-16}$ - 10^{-15}
Ceramic	2000-3000	10^{-16} - 10^{-15}

Figure 9: Hardness and specific wear factor for different materials coupled with high-strength steel (adapted from [10])

The value K_a is expressed in SI units in m^2/N, resulting in extremely small values; to make these value easier to manage in the Archard's equation, a change to

multiples of the fundamental units leads to an easier physical interpretation. Considering for example a value of $K_a = 1 \cdot 10^{-15}$ m^2/N = 1.0 mm^3/[km kN]. This means that 1 mm^3 of material is removed when the surfaces are subjected to 1 kN of *normal* force and they slide for 1 km. Please note that this force is different from that described at par. 3.3 where *tangential* (*sliding*) force is considered.

The value of K_a is extremely variable and it depends not only on the material involved in the wear process, but also on the mechanism of wear, usually divided in *mild wear* and *severe wear*.

Figure 10 shows how the value of K_a for grey cast iron changes by approximately two orders of magnitude with the nominal contact pressure, passing from mild wear to severe wear. The pressure on cones active surface is nominally 1.1 MPa (external surface) and 1.8 MPa (internal surface), but as long as wear is greater where the pressure is higher, it is reasonable to suppose that quite soon the pressure will assume the average value ≅ 1.45 MPa.

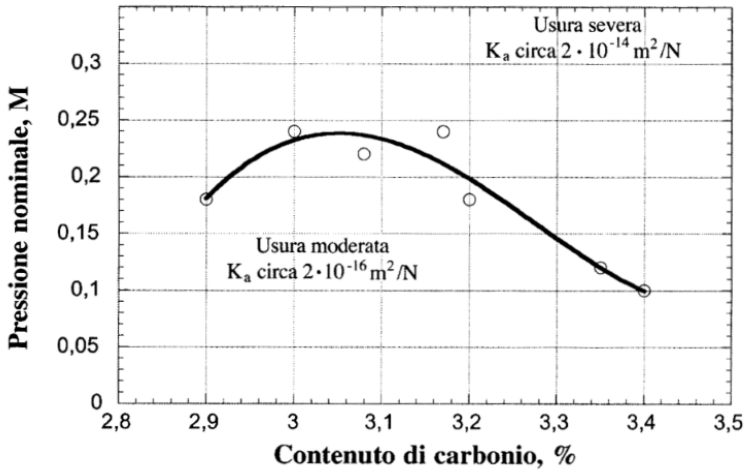

Figure 10: Moderate and severe wear for grey cast iron as a combination of nominal pressure (y-axis, [MPa]) and carbon content (x-axis, [%]). Moderate wear K_a=2·10^{-16} m^2/N, severe wear K_a=2·10^{-14} m^2/N (from [10]).

This value is in the range of severe wear for grey cast iron but it is known that spheroidal cast iron possesses superior performances for high pressures and slow motion ([10], p. 160). As an example, big valve castings in the energy (oil & gas) industry are often made of spheroidal graphite cast iron as it doesn't seize even for small angles at low angular speed.

As no data were found for spheroidal graphite cast iron, an intermediate value of $K_a = 2 \cdot 10^{-15}$ m^2/N = 2 mm^3/[km kN] derived from grey cast iron properties was chosen, limiting the maximum radial wear to 1.5 mm. This results in an "axial deepening" of the cones of 5.8 mm. This value was set with the aim of limiting the

decrease in the axial force given by the coil springs used. About these springs, their choice was a compromise between a low stiffness (to keep the force as constant as possible even during wear of the discs) and practical mounting considerations (too long springs tend to buckle and can damage and be dangerous for operators).

With these solutions the estimated life for the torque limiter when applied to a vehicle running on the Sardinian backbone network (Sections 1+2) is around 5.5 million km depending, a life that seems sufficient for a railway application. The variation in the intervention torque due to discs wear, is lower than ±8% but can be further reduced to ±4% by the use of shims that can be removed after a half worn condition is reached. This solution is not shown here for brevity but it is quite simple to implement.

5 Conclusions and further developments

A careful analysis led to the conclusion that the torque limiter to be applied on the *AIR wheelset* doesn't exist on the market. It was therefore decided to design a fully passive, simple and low-cost spring-loaded torque limiter capable to supply the desired torque and to last for many million kilometres.

The study has some weak points. First of all the calculation on the torque and the dissipated power were obtained by crossing the data from a simulation performed on the Sardinian backbone line for the ERRI wagon while the speed of the vehicle was obtained from the simulation of a DMU vehicle. So, there may be some differences between the actual interventions of the torque limiter and the estimated ones.

The second weak point is the absence of real data on the specific wear between spheroidal graphite cast iron and hard steel; it is supposed in this work that wear will be lower than that for grey cast iron, but this must be confirmed.

Last but not least, an experimental verification of the properties of the proposed torque limiter in terms of durability and real behaviour is missing.

It can be concluded, anyway, that the design looks simple and robust enough to make the practical implementation hopefully durable and reliable.

References

[1] AB Consulting sas di Andrea Bracciali & C., "Railway Wheelset With Partially Independent Wheels", International patent PCT/IB2015/051855 (13.03.2015), European patent EP15173213.8 (22.06.2015).

[2] A. Bracciali, "Apparently Independently Rotating Wheelset - a possible solution for all needs?", The Stephenson Conference - Research for Railways, Institution of Mechanical Engineers, London, 23-25 April 2015.

[3] A. Bracciali, G. Megna, “Running dynamics of railway vehicles equipped with torsionally flexible axles and partially independently rotating wheels”, 24th IAVSD, Graz, Austria, 17-21 August 2015.
[4] A. Bracciali, G. Megna: “Contact Mechanics Issues Of A Vehicle Equipped With Partially Independently Rotating Wheelsets”, Contact Mechanics 2015 Conference, 30.8-3.9.2015, Colorado Springs, USA.
[5] A. Bracciali Andrea, P. Cavicchi, A. Corbizi Fattori, “Maintainability of wheelsets: a novel solution to save time and money”, submitted to 11th World Congress on Railway Research 2016, Milan, Italy, 29.5-2.6.2016.
[6] A. Bracciali: “Recent developments in railway wheelset: impacts on safety, maintenance and LCC”, invited opening lecture at The Third International Conference on Railway Technology: Research, Development and Maintenance, Cagliari, Italy, 5-8.4.2016
[7] A. Bracciali, F. Piccioli, T. De Cicco: “Wear and RCF behaviour of conventional and hard rails in different contexts”, Proceedings of Railway Engineering 2009 Conference, London, 24-25 June 2009 (on CD).
[8] U. Olofsson, R. Lewis, "Tribology of the Wheel- Rail Contact", in S. Iwnicki (ed.), Handbook of Railway Vehicle Dynamics, CRC Press, ISBN 978-0-8493-3321-7
[9] D. Thompson, Railway Noise and Vibration - Mechanism, Modelling and Means of Control, Elsevier, 2009, ISBN-13: 978-0-08-045147-3.
[10] G. Straffelini, “Attrito e usura. Metodologie di progettazione e controllo”, Editore Tecniche Nuove, Milano, 2005.